



Article

Correlative Dynamics of Complex Systems: A Multifractal Perspective of Motion Based on $SL(2R)$ Symmetry

Vlad Ghizdovat ¹, Emanuel Nazaretian ², Catalin Gabriel Dumitras ², Maricel Agop ^{3,4,*}, Constantin Placinta ⁵, Calin Buzea ⁶, Cristina Marcela Rusu ³, Decebal Vasincu ⁷ and Zoltan Borsos ⁸

- ¹ Biophysics and Medical Physics Department, “Grigore T. Popa” University of Medicine and Pharmacy, 700115 Iasi, Romania; vlad.ghizdovat@umfiasi.ro
- ² Faculty of Machine Manufacturing and Industrial Management, “Gheorghe Asachi” Technical University, 700050 Iasi, Romania; emanuel.nazaretian@tuiasi.ro (E.N.); catalin-gabriel.dumitras@academic.tuiasi.ro (C.G.D.)
- ³ Physics Department, “Gheorghe Asachi” Technical University, Prof. dr. docent Dimitrie Mangeron Rd., No. 59A, 700050 Iasi, Romania; cristina.rusu@tuiasi.ro
- ⁴ Academy of Romanian Scientists, 3 Ilfov, 050044 Bucharest, Romania
- ⁵ Faculty of Material Science and Engineering, “Gheorghe Asachi” Technical University, 700050 Iasi, Romania; constantin.placinta@tuiasi.ro
- ⁶ National Institute of Research and Development for Technical Physics, 700050 Iasi, Romania; picardout@phys-iasi.ro
- ⁷ Biophysics Department, Faculty of Dental Medicine, “Grigore T. Popa” University of Medicine and Pharmacy, 16 University Str., 700115 Iasi, Romania; decebal.vasincu@umfiasi.ro
- ⁸ Information Tehnology, Informatics, Mathematics and Physics Department, Faculty of Letters and Sciences, Petroleum-Gas University of Ploiesti, No. 39 Bucuresti Blv., 100680 Ploiesti, Romania; borzolh@upg-ploiesti.ro
- * Correspondence: magop@tuiasi.ro

Abstract: By assimilating any complex system into a multifractal, a new approach for describing the dynamics of such systems is proposed by means of the Multifractal Theory of Motion. In such context, the description of these dynamics is accomplished through continuous and non-differentiable curves (multifractal curves), giving rise to two scenarios. The first scenario is a Schrödinger-type multifractal scenario, a situation in which the motion laws can be related to the $SL(2R)$ algebra invariant functions. The second scenario is a Madelung-type multifractal scenario, a situation in which if the differentiable and non-differentiable components of the velocity field satisfy a particular restriction, an $SL(2R)$ symmetry can also be highlighted. Moreover, correlative dynamics in either of the two scenarios, based on the same $SL(2R)$ symmetry, can be obtained by Riccati-type gauges, which imply Stoler coherent states. Several cases induced by the $SL(2R)$ symmetry are also analyzed.

Keywords: complex systems; $SL(2R)$ symmetry function; Multifractal Theory of Motion; Riccati-type gauge



Academic Editor: Quanxin Zhu

Received: 26 November 2024

Revised: 21 December 2024

Accepted: 25 December 2024

Published: 27 December 2024

Citation: Ghizdovat, V.; Nazaretian, E.; Dumitras, C.G.; Agop, M.; Placinta, C.; Buzea, C.; Rusu, C.M.; Vasincu, D.; Borsos, Z. Correlative Dynamics of Complex Systems: A Multifractal Perspective of Motion Based on $SL(2R)$ Symmetry. *Symmetry* **2025**, *17*, 27. <https://doi.org/10.3390/sym17010027>

Copyright: © 2024 by the authors. Licensee MDPI, Basel, Switzerland. This article is an open access article distributed under the terms and conditions of the Creative Commons Attribution (CC BY) license (<https://creativecommons.org/licenses/by/4.0/>).

1. Introduction

The manifestation of a complex system cannot be anticipated just by the behavior of its constituent components or by aggregating their behaviors. Rather, it is dictated by the manner in which the structural units interact to affect global behavior. Key characteristics of these systems include emergence, self-organization, and adaptability, among others [1–3]. Complex systems are exemplified in human societies, the brain, the internet, ecosystems, biological evolution, financial markets, and economics, among others [4,5].

Consequently, the theoretical models describing the dynamics of complex systems have grown more sophisticated [6–8]. Nonetheless, the situation may be standardized

by acknowledging that the intricacy of the interaction process demands varied temporal resolution scales, and the development of patterns imposes different degrees of freedom [2].

To formulate new theoretical models, we must acknowledge that complex systems exhibiting chaotic behavior are known to acquire self-similarity, with space-time patterns emerging alongside significant fluctuations at all conceivable space-time scales [1–3]. For extensive temporal scales relative to the inverse of the largest Lyapunov exponent, deterministic trajectories are substituted by a set of possible trajectories, and the notion of definite positions is replaced by that of probability density. One of the most intriguing instances is the collision processes in complex systems, where the dynamics of the particles may be characterized by non-differentiable curves [9,10].

Given that non-differentiability is a universal characteristic of complex systems, it is essential to develop a non-differentiable physics. In this hypothesis, by assuming that the complexity of interaction processes is replaced by non-differentiability, it becomes unnecessary to use the whole classical repertoire of quantities from conventional physics (differentiable physics).

This subject was formulated under the Scale Relativity Theory (SRT) [11] and the Multifractal Theory of Motion (MTM), i.e., the Scale Relativity Theory including an arbitrary constant fractal dimension [12]. Within the context of SRT or MTM, we consider that the movements of complex system entities occur along continuous but non-differentiable curves (multifractal curves), such that all physical phenomena associated with the dynamics are contingent not only on the space-time coordinates but also on the resolution of space-time scales. From this viewpoint, the physical characteristics describing the behavior of complex systems may be seen as multifractal functions [11,13]. Furthermore, the components of the complex system may be reduced to and identified with their respective trajectories, allowing the system to function as a unique interaction-less “fluid” via its geodesics in a non-differentiable (multifractal) space (Schrödinger or hydrodynamic representations).

This study presents a novel methodology for characterizing the dynamics of complex systems within the context of the Multifractal Theory of Motion. We start by assimilating any complex system to a mathematical object of multifractal type. In this way, the characterization of complex systems dynamics is achieved by continuous and non-differentiable curves (multifractal curves), resulting in two scenarios. The first scenario is a Schrödinger-type multifractal scenario, in which the motion laws can be related to the SL(2R) algebra invariant functions. The second scenario is a Madelung-type multifractal scenario, in which the non-differentiable components of the velocity field manifest as a gradient of a scalar function. These two scenarios are correlative, highlighting SL(2R) invariances (i.e., symmetry induced by the SL(2R) groups) and Riccati-type gauges in such dynamics. Several cases are presented.

2. Multifractal Covariant Derivative and Conservation Laws

Let us admit that complex systems can be assimilated into a multifractal type of mathematical object. If, in such context, we agree to describe any complex system dynamics through continuous and non-differentiable curves (multifractal curves), then, according to the Multifractal Theory of Motion [12], the standard operator d/dt must be substituted with the operator \hat{d}/dt (with the role of covariant derivative), in the following form:

$$\frac{\hat{d}}{dt} = \partial_t + \hat{V}^l \partial_l - i\lambda(dt)^{[\frac{2}{f(\omega)} - 1]} \partial^l \partial_l, \quad i = \sqrt{-1}, \quad l = 1, 2, 3 \quad (1)$$

$$\hat{V}^l = V_D^l - iV_F^l \quad (2)$$

$$\partial_t = \frac{\partial}{\partial t}, \quad \partial_l = \frac{\partial}{\partial x^l}, \quad \partial^l \partial_l = \frac{\partial^2}{\partial x_l^2} \quad (3)$$

In relations (1)–(3), \hat{V}^l is the velocity component at global scale resolution (we will call it global velocity), V_D^l is the velocity component at differentiable scale resolution (we will call it differentiable velocity), V_F^l is the velocity component at non-differentiable scale resolution (we will call it non-differentiable velocity), x_l is the multifractal spatial coordinate, t is the non-multifractal temporal coordinate, λ is a coefficient associated with the multifractal–non-multifractal transition, $f(\alpha)$ is the singularity spectrum of order $\alpha \equiv \alpha(D_F)$ for motion curves in the fractal dimension D_F , and dt is the scale resolution. From such a perspective, by using $f(\alpha)$, we gain the following advantages:

- (i) The presence of a prevailing fractal dimension in any complex system dynamics allows for the identification of a global pattern. The explication of such a pattern becomes compatible with global structuralities and functionalities, specific only to monofractal dynamics;
- (ii) The presence of fractal dimensions “set” in any complex system dynamics allows the identification of zonal patterns. The explication of such patterns becomes compatible with local structuralities and functionalities, specific only to multifractal dynamics;
- (iii) Through the functionality of the singularity spectrum of order α , universality classes can be identified in any complex system dynamics, even in the case in which the attractors associated with these dynamics have different aspects.

Now, also according to the Multifractal Theory of Motion [12], the dynamics of a complex system can be explicated based on the following scale covariance principle: the motion laws of any complex system are invariant, both in relation with space-time coordinates transformation, and in relation with scale resolution transformations.

In this framework, for example, the specific momentum conservation law at global scale resolution has the following form:

$$\frac{d\hat{V}^p}{dt} = \partial_t \hat{V}^p + \hat{V}^l \partial_l \hat{V}^p - i\lambda(dt)^{[\frac{2}{f(\alpha)}-1]} \partial^l \partial_l \hat{V}^p = 0, \quad p = 1, 2, 3 \quad (4)$$

Now, by separating dynamics on scale resolution, we can obtain the following:

$$\frac{dV_D^i}{dt} = \partial_t V_D^i + V_D^l \partial_l V_D^i - \left[V_F^i + \lambda(dt)^{[\frac{2}{f(\alpha)}-1]} \partial^l \right] \partial_l V_F^i = 0 \quad (5)$$

at differentiable scale resolution, and

$$\frac{dV_F^i}{dt} = \partial_t V_F^i + V_D^l \partial_l V_F^i + \left[V_F^l + \lambda(dt)^{[\frac{2}{f(\alpha)}-1]} \partial^l \right] \partial_l V_D^i = 0 \quad (6)$$

at non-differentiable scale resolution.

3. Dynamics Analysis Scenarios

In particular, for irrotational dynamics expressed through constraints:

$$\varepsilon_{ilk} \hat{V}^k = 0 \quad (7)$$

where ε_{ilk} is Levi–Civita’s pseudotensor, a complex scalar potential for the velocities field can be defined as follows:

$$\hat{V}^i = -2i\lambda(dt)^{[\frac{2}{f(\alpha)}-1]} \partial^l \ln \psi \quad (8)$$

where ψ is the multifractal state function. From here, two scenarios for describing any complex system’s dynamics become viable:

- (i) a Schrödinger multifractal scenario explicated through the differential equation (for details see [12]):

$$\lambda^2(dt)^{[\frac{4}{f(\alpha)}-2]}\partial^l\partial_l\psi + i\lambda(dt)^{[\frac{2}{f(\alpha)}-1]}\partial_t\psi = 0 \quad (9)$$

Let us note that, for complex systems monofractal dynamics characterized by Peano-type curves at fractal dimension $D_F = 2$ [12] and at Compton scale resolution, $\lambda = \hbar/2m_0$ (where \hbar is the reduced Planck constant and m_0 is the microparticle's rest mass), Equation (9) is reduced to Schrödinger's differential equation from Quantum Mechanics;

(ii) a Madelung multifractal scenario explicated through the multifractal hydrodynamics differential equations system (for details see [12]):

$$\begin{aligned} \partial_t V_D^i + (V_D^l \partial_l) V_D^i &= -\partial^i Q \\ \partial_t \rho + \partial^i (\rho V_D^i) &= 0 \end{aligned} \quad (10)$$

with

$$\begin{aligned} Q &= -2\lambda^2(dt)^{[\frac{4}{f(\alpha)}-2]}\frac{\partial^l\partial_l\sqrt{\rho}}{\sqrt{\rho}} = -\frac{V_F^l V_{Fl}}{2} - \lambda(dt)^{[\frac{2}{f(\alpha)}-1]}\partial_i V_F^i \\ V_D^i &= 2\lambda(dt)^{[\frac{4}{f(\alpha)}-2]}\partial^i\phi, \quad V_F^i = \lambda(dt)^{[\frac{2}{f(\alpha)}-1]}\partial^i\phi \\ \psi &= \sqrt{\rho}e^{i\phi}, \quad \bar{\psi} = \sqrt{\rho}e^{-i\phi}, \quad \rho = \psi\bar{\psi}, \end{aligned} \quad (11)$$

$\sqrt{\rho}$ the amplitude and ϕ the phase of the state function. The first Equation (10) corresponds to the specific multifractal momentum conservation law, while the second Equation (10) corresponds to the multifractal states density conservation law. From such a perspective, several consequences can be highlighted: (a) any complex system identifies as a non-differentiable fluid (multifractal fluid), its dynamics being described through the multifractal hydrodynamics equations system; (b) any complex system structural entity is in permanent interaction with a multifractal medium by means of specific multifractal potential Q ; (c) the absence of v_F^l from the multifractal states density conservation law specifies that it does not intervene in the actual motion, but contributes both to the specific multifractal momentum transfer and to the multifractal energy transfer; (d) any interpretation of Q must take into account the self-interactive nature of specific multifractal momentum transfer. In this framework, if we admit for the first Equation (10) the general form:

$$\partial_t v_D^i + (v_D^l \partial_l) v_D^i = -\partial^i (Q + U), \quad (12)$$

where U is the specific multifractal scalar potential, from Equation (12), the multifractal energy conservation law can be obtained for dynamical states ($\partial_t = 0, v_D^i \neq 0$):

$$\frac{1}{2}v_D^i v_{Di} + U + Q = E = \text{const.} \quad (13)$$

It follows that, while a part of the multifractal energy is stored, both in the form of a specific multifractal kinetic energy, $\frac{1}{2}v_D^i v_{Di}$, and in the form of a specific multifractal potential energy, U , other parts are available in the form of Q and only the total multifractal energy is conserved. In this way, by means of the multifractal momentum and energy conservation laws, the multifractal reversibility and the existence of multifractal eigenstates are assured; (d) in the case of complex systems monofractal dynamics described through Peano-type curves in the fractal dimension $D_F = 2$ [12] and at Compton scale resolution, $\lambda = \hbar/2m_0$, Equation (10) are reduced to the quantum hydrodynamics differential equation system [12].

4. Correlative Dynamics by Means of Two Scenarios

In its usual vectorial form, at a given scale resolution, the Schrödinger multifractal equation, besides the fact that it is invariant with respect to a Galilean-type group, it is also invariant, in a separate way, to time and radial coordinates transformations (which represent a group in themselves [12]). They constitute, in the most general case of motion in a singular direction [10–12], a realization of the Lie SL(2R) group structure, in two variables with 3 parameters, by the following action:

$$t \rightarrow \frac{\alpha t + \beta}{\gamma t + \delta}, \quad r \rightarrow \frac{r}{\gamma t + \delta} \quad (14)$$

$$\alpha, \beta, \gamma, \delta \in \mathbb{R}$$

The Lie SL(2R) algebra corresponding to action (14) of the group is given by the following vector base which acts in two variables:

$$\hat{X}_1 = \frac{\partial}{\partial t}, \quad \hat{X}_2 = t \frac{\partial}{\partial t} + \frac{r}{2} \frac{\partial}{\partial r}, \quad \hat{X}_3 = t^2 \frac{\partial}{\partial t} + tr \frac{\partial}{\partial r} \quad (15)$$

These differential operators satisfy the typical SL(2R) algebra's commutative relations:

$$[\hat{X}_1, \hat{X}_2] = \hat{X}_1, \quad [\hat{X}_2, \hat{X}_3] = \hat{X}_3, \quad [\hat{X}_3, \hat{X}_1] = -2\hat{X}_3 \quad (16)$$

An invariant function is canceled by the algebra's general vector and thus is dependent on three arbitrary constants.

If $F(t, r)$ is such a function, it must represent a solution of the partial derivatives equation:

$$(a_3 \hat{X}_1 + 2a_2 \hat{X}_2 + a_1 \hat{X}_3)(F) = 0 \quad (17)$$

or explicitly,

$$(a_1 t^2 + 2a_2 t + a_3) \frac{\partial F}{\partial t} + (a_1 t + a_2) \frac{\partial F}{\partial r} = 0 \quad (18)$$

Therefore, it must be a continuous function of an algebraic expression:

$$F(r, t) = \frac{r^2}{a_1 t^2 + 2a_2 t + a_3} \quad (19)$$

In the particular case in which such a function is a constant (for example, $F(r, t) \equiv 1$), it results the following:

$$r^2 = a_1 t^2 + 2a_2 t + a_3 \quad (20)$$

Equation (20) is indeed the radial motion equation of a free particle, with position represented by a linearly time-dependent vector, according to classical dynamics. In this interpretation, a_1 is the square of the initial velocity vector, a_2 is the scalar product of the initial velocity and the initial position vector, and a_3 is the square of the initial position vector. This radial motion is a prototype in displaying the modern idea of the "dynamics reduction procedure", through which certain dynamics are presented as cinematics of special freedom degrees [14]. We must also note that Equation (20), as a classical motion equation, represents non-trivial dynamics with significant radial motion: the motion of a charged particle in the field of a magnetic monopole—the so-called Poincaré monopole [15]. In the context of an "ensemble of motions", and therefore in the context of fractalization through stochasticization, these dynamics display, by means of the Multifractal Theory of Motion, a special interpretation, from a cosmological point of view.

Eddington showed that, from a cosmological perspective, r^2 can be interpreted as a standard particle Gaussian ensemble variance that characterizes the relativistic uni-

verse [16]. This fact suggests a general way of seeing things. Equation (20) can indeed represent a variance in the time moments ensemble corresponding to the concept of the same scale resolution. In this case, its interpretation is general, in the sense that it is independent from Kepler's second law, due to the fact that Equation (20), in the form

$$\frac{dt}{d\theta} = a_1 t^2 + 2a_2 t + a_3, \quad (21)$$

represents in fact the connection between the average and the variance of the most general ensembles employed in current physics, i.e., exponential ensembles with a quadratic variance function [17]. Among these, the Gaussian ensembles from Eddington's work are only a particular case.

In this way, the time parameter t has the interpretation of an average on-time moments ensembles corresponding to a value of the parameter θ which is characteristic of the statistical distribution of variance r^2 . In the case of motion in the multifractal potential Q , parameter θ is the polar angle of the sample body's position, the angle in relation to which the $r(t) = \text{const.}$ ensemble "unfolds" along the sample body's closed orbit. On the other hand, the cosmological perspective helps in placing the previous statistical interpretation among the special reduction procedure mentioned above. It is now necessary to remind an older idea, related to the changing of the time scale [18]. Indeed, Equation (21) can be adequately solved by providing t as a function of θ parameter. Now, if parameter θ is itself taken as a time, let us consider, for example, the choice $\theta = k^{-1}\tau$, $k = \text{const.}$ (a fixed time in a certain time scale), then the solution of Equation (21) represents different time scales, Milne's scale is one of them. Let us analyze in detail this situation. In this framework, Equation (21), with adequate normalization and notations $b_i = ka_i$, $i = 1, 2, 3$, is transformed into a Riccati-type differential equation (Riccati-type gauge):

$$\frac{dt}{d\tau} = P(t), \quad P(t) = b_1 t^2 + 2b_2 t + b_3 \quad (22)$$

Here, the parameters, b_i are constants that characterize a certain geodesic of the family. Let us note that, a choice like (22) highlights correlations between the dynamics present in the two above-mentioned multifractal scenarios (the Schrödinger multifractal scenario gives us the invariant function, through the $SL(2R)$ symmetry group, taking into account that the Madelung multifractal scenario gives us the force field's centrality).

For obvious reasons, it is important to identify the most general solution of the differential Equation (22). Reference [19] offers a modern and pertinent method for the integrability of the Riccati differential equation. For the present work, it is sufficient to note that the relations:

$$t_1 = -\frac{b_2}{b_1} + \frac{i}{b_1}\omega, \quad t_2 = -\frac{b_2}{b_1} - \frac{i}{b_1}\omega, \quad \omega^2 = b_3 b_1 - b_2^2, \quad i = \sqrt{-1} \quad (23)$$

can be assimilated to the roots of the polynomial $P(t)$. As such, the homographic transformation needs to be performed first:

$$z = \frac{t - t_1}{t - t_2} \quad (24)$$

and now it is easy to see, by means of direct calculation, that z is a solution of the differential equation:

$$\dot{z} = 2i\omega z, \quad z(\tau) = z(0)e^{i\omega\tau} \quad (25)$$

Therefore, if the initial condition $z(0)$ is conveniently expressed, it is possible to obtain the general solution of the differential Equation (22), by inverting the transformation (24), which implies (i.e., the solution):

$$t = \frac{t_1 + r \exp[2i\omega(\tau - \tau_0)]t_2}{1 + r \exp[2i\omega(\tau - \tau_0)]} \quad (26)$$

where r and τ_0 are two real constants, specific to the solution.

By using relations (23), it is possible to obtain the solution in real terms, as follows:

$$z = -\frac{b_2}{b_1} + \frac{\omega}{b_1} \left[\frac{2r \sin[2\omega(\tau - \tau_0)]}{1 + r^2 + 2r \cos[2\omega(\tau - \tau_0)]} + i \frac{1 - r^2}{1 + r^2 + 2r \cos[2\omega(\tau - \tau_0)]} \right] \quad (27)$$

resulting in a self-modulation of ω through the Stoler-type transformation (usually referred to as Stoler coherent states [20]), leading to a complex form of this complex parameter. We present, in Figure 1, the explication of “self-modulation” in complex systems dynamics, based on Equation (27), through $Re(zb_1 + b_2; b_1 = b_2 \equiv 1)$, for $\omega = 17$ and $r = 0.2; 0.6; 1$.

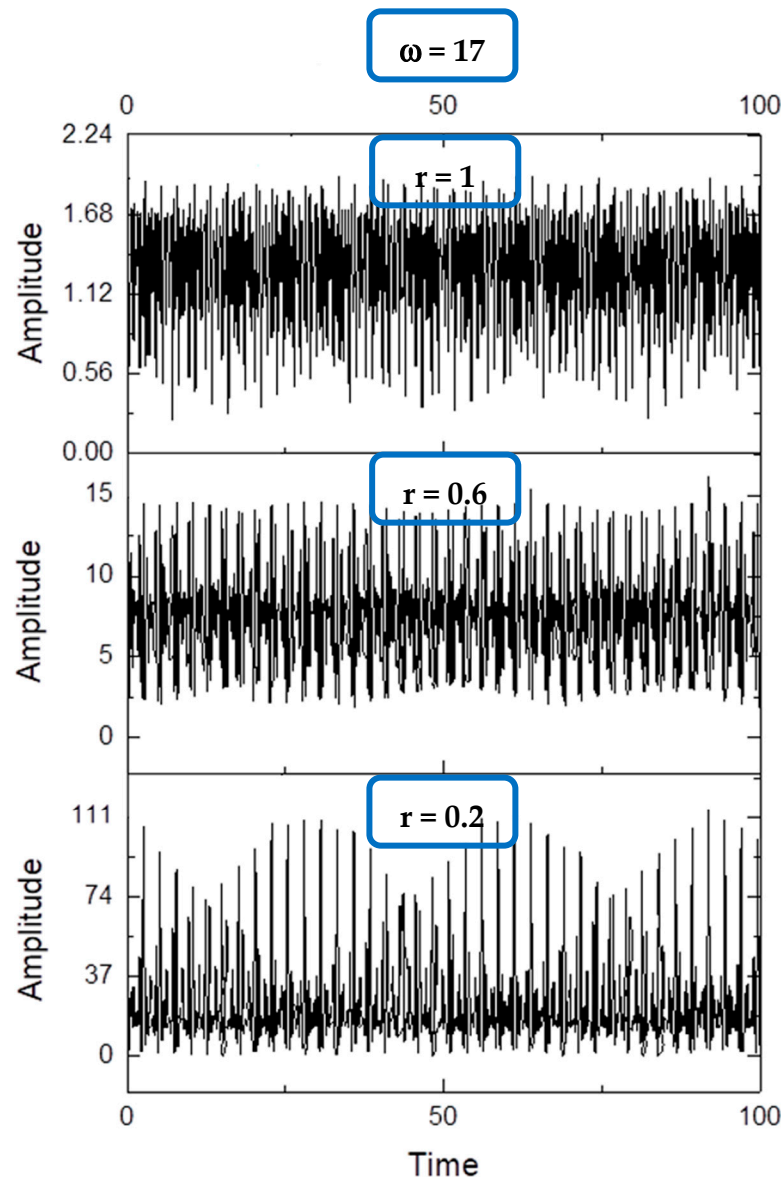


Figure 1. “Self-modulation” in complex systems dynamics through $Re(zb_1 + b_2; b_1 = b_2 \equiv 1)$, for $\omega = 17$ and $r = 0.2; 0.6; 1$.

Moreover, if we write:

$$r = \coth s \quad (28)$$

then Equation (20) becomes:

$$z = -\frac{b_2}{b_1} + \frac{\omega}{b_1} h \quad (29)$$

where h has the expression

$$h = -i \frac{\cosh s - \exp[-2i\omega(\tau - \tau_0)] \sinh s}{\cosh s + \exp[-2i\omega(\tau - \tau_0)] \sinh s} \quad (30)$$

5. Correlative Dynamics by Means of Schrödinger Multifractal Scenario

Let us reconsider the first Equation (14), which represents the homographic action of the generic matrix:

$$\hat{M} = \begin{pmatrix} \alpha & \beta \\ \gamma & \delta \end{pmatrix} \quad (31)$$

The issue that needs to be tackled is the following: a relation must be found between the ensemble of matrices \hat{M} and the ensemble of values pertaining to t , for which t' remains constant.

From a geometric perspective, this means finding the ensemble of points $(\alpha, \beta, \gamma, \delta)$, which univocally correspond to the values of the parameter t . By using the first Equation (14), the issue is solved by a Riccati differential equation (Riccati-type gauge), which can be obtained as a consequence of the constancy of t' : $dt' = 0$.

$$dt + \omega_1 t^2 + \omega_2 t + \omega_3 = 0 \quad (32)$$

where the following notations are used [12,19]:

$$\omega_1 = \frac{\gamma d\alpha - \alpha d\gamma}{\alpha\delta - \beta\gamma}, \quad \omega_2 = \frac{\delta d\alpha - \alpha d\delta + \gamma d\beta - \beta d\gamma}{\alpha\delta - \beta\gamma}, \quad \omega_3 = \frac{\delta d\beta - \beta d\delta}{\alpha\delta - \beta\gamma} \quad (33)$$

It is then easily noticeable that the metric

$$ds^2 = \frac{(\alpha d\delta + \delta d\alpha - \beta d\gamma - \gamma d\beta)^2}{4(\alpha\delta - \beta\gamma)^2} - \frac{d\alpha d\delta - d\beta d\gamma}{\alpha\delta - \beta\gamma} \quad (34)$$

is in direct relation with the discriminant of the quadratic polynomial from Equation (32)

$$ds^2 = \frac{1}{4} (\omega_2^2 - 4\omega_1\omega_3) \quad (35)$$

Let us note that, for a particular case of 1-forms $\omega_1, \omega_2, \omega_3$ [12], the metric (35) also admits the SL(2R) symmetry.

The three differential forms from Equation (33) constitute a coframe [12] at any point of the absolute space. This allows the translation of the geometric properties of the absolute space to algebraic properties linked to the differential Equation (32).

The simplest of these properties refer to dynamics on matrix geodesics, which are directly translated to statistical properties. In this case, the 1-forms $\omega_1, \omega_2, \omega_3$ are differentiated exactly in the same parameter the length l of the geodesic arc. Along these geodesics, Equation (32) is transformed into a Riccati-type differential equation (Riccati-type gauge):

$$\frac{dt}{dl} = P(t), \quad P(t) = c_1 t^2 + 2c_2 t + c_3 \quad (36)$$

We can notice that such a situation implies in-phase correlative dynamics of complex systems.

Here, the parameters c_1, c_2, c_3 are constants that characterize a certain geodesic of the family. The formalism employed for Equation (22) can also be applied to this equation. In this case, Equation (36) highlights dynamics correlated by Stoler coherent states. Let us note the similarities between the dynamics given by Equations (22) and (36), due to the fact that both are substantiated by the $SL(2R)$ symmetry group [12,20].

In accordance with [9,10], the complex parameter (30) operates as a harmonic mapping between the usual space (i.e., the measurement space) and the hyperbolic one.

We present in Figure 2a–d chaotic in complex systems dynamics, based on Equation (27), through $Re(zc_1 + c_2; c_1 = c_2 \equiv 1) \equiv F(\omega, t)$ for $\omega_{max} = 13$.

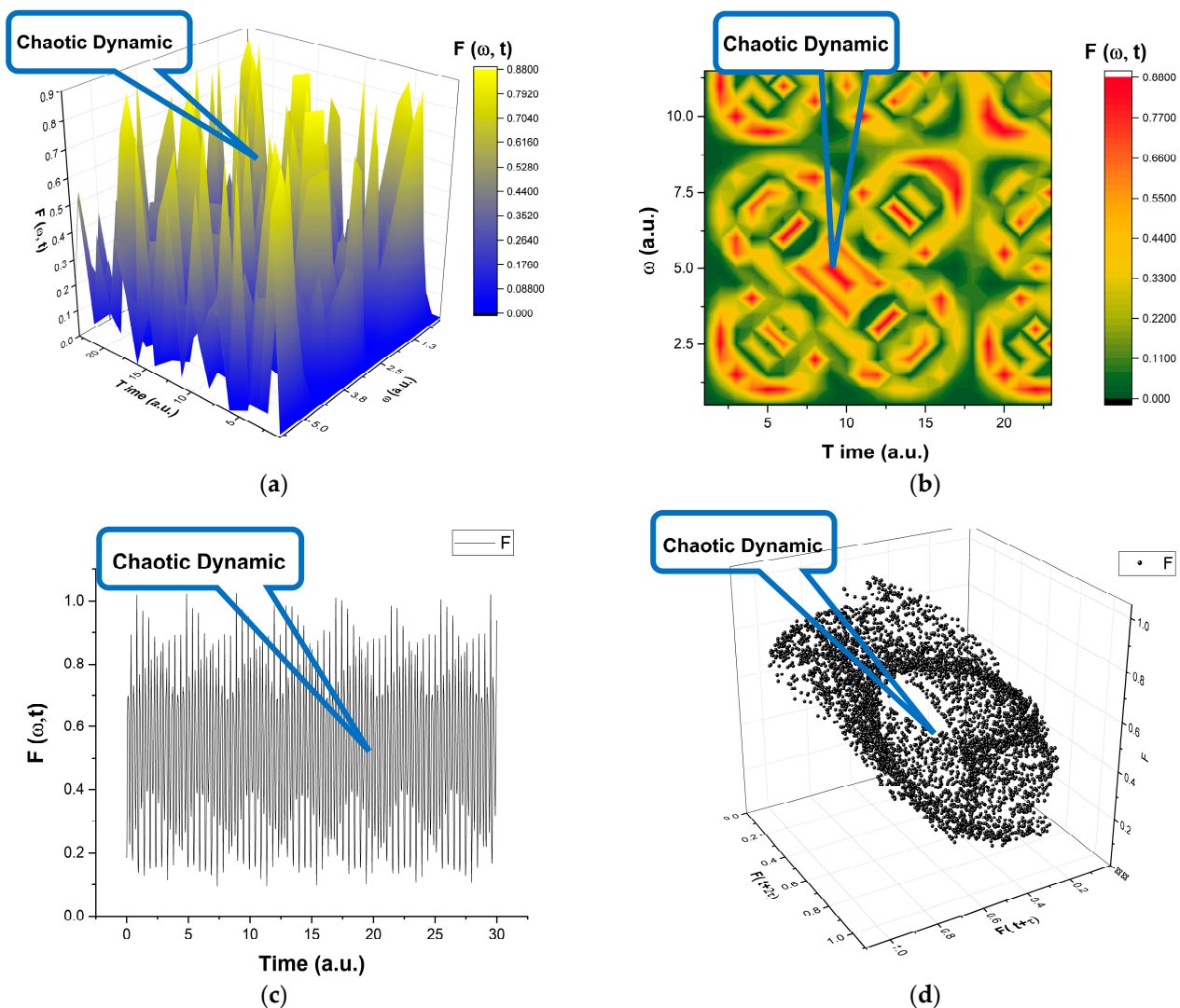


Figure 2. (a,b)—3D plot (a), contour plot (b), time series (c), and reconstructed attractor (d) for solution $Re(zc_1 + c_2; c_1 = c_2 \equiv 1) \equiv F(\omega, t)$ corresponding to the maximum value of the pulsation-type characteristic $\omega_{max} = 13$.

6. Correlative Dynamics by Means of Madelung Multifractal Scenario

Let us suppose that the velocity field is described by the variables (Y^j) , for which we have the metric:

$$h_{ij}dY^i dY^j \quad (37)$$

in an ambient space of metric:

$$\gamma_{\alpha\beta} dx^\alpha dx^\beta \quad (38)$$

In this situation, the velocity field equations are derived from a variational principle, connected to the Lagrangian [12]:

$$L = \gamma^{\alpha\beta} h_{ij} \frac{\partial Y^i}{\partial x^\alpha} \frac{\partial Y^j}{\partial x^\beta} \quad (39)$$

Therefore, if the variational principle

$$\delta \int L dv = 0 \quad (40)$$

where the quantities have the standard meaning from [12], is considered as a fundamental premise, the main purpose in the dynamics of complex systems would be to produce metrics of the Lobachevsky plane (or related to them).

In such a framework, let us admit that, in the case of one-dimensional dynamics of the velocity field, the restriction:

$$V_D^2 + V_F^2 \equiv 1 \quad (41)$$

Indeed, the metric of the Lobachevsky plane can be produced as a Cayleyan metric of a Euclidian plane, for which the absoluteness is a circle with unit radius:

$$x^2 + y^2 = 1 \quad (42)$$

where we admitted the following:

$$x \equiv V_D, y \equiv V_F \quad (43)$$

This way, the Lobachevsky plane can be put into biunivoc correspondence with the interior side of this circle. The general procedure of metrization of a Cayleyan space starts with the definition of the metric as an anharmonic ratio [12].

Let us suppose that the absoluteness of the space is represented by the quadratic form $\Omega(X, Y)$ where X denotes any vector. The Cayleyan metric is then given by the following differential quadratic form:

$$\frac{ds^2}{k^2} = \frac{\Omega(dX, dX)}{\Omega(X, X)} - \frac{\Omega^2(X, dX)}{\Omega^2(X, X)} \quad (44)$$

where $\Omega(X, Y)$ is the duplication of $\Omega(X, X)$ and k is a constant connected to the space curvature.

In the case of the Lobachevsky plane, we have the following:

$$\begin{aligned} \Omega(X, X) &= 1 - x^2 - y^2, \\ \Omega(X, dX) &= -x dx - y dy \\ \Omega(dX, dX) &= -dx^2 - dy^2 \end{aligned} \quad (45)$$

which yields:

$$\frac{ds^2}{k^2} = \frac{(1 - y^2) dx^2 + 2xy dx dy + (1 - x^2) dy^2}{(1 - x^2 - y^2)^2} \quad (46)$$

Performing now the coordinate transformation:

$$x = \frac{h\bar{h} - 1}{h\bar{h} + 1}, \quad y = \frac{h + \bar{h}}{h\bar{h} + 1} \quad (47)$$

the metric (46) becomes as follows:

$$\frac{ds^2}{k^2} = -4 \frac{dh d\bar{h}}{(h - \bar{h})^2} \quad (48)$$

Let us note that this metric admits a symmetry of SL(2R) type [12].

In such context, by applying the variational principle (40) to the Lagrangean

$$L = -4 \frac{\nabla h \nabla \bar{h}}{(h - \bar{h})^2} \quad (49)$$

where \bar{h} is the complex conjugate of h , the following field equations can be found the following:

$$(h - \bar{h}) \nabla^2 h - 2(\nabla h)^2 = 0 \quad (50)$$

These equations have the solution

$$h = i \frac{\cos h\kappa + \sin h\kappa e^{-i\omega}}{\cos h\kappa - \sin h\kappa e^{-i\omega}} \quad (51)$$

where κ satisfies the Laplace equation $\Delta \kappa = 0$. Therefore, also in this case, the complex parameter (50) operates as a harmonic mapping between the usual space (i.e., the measurement space) and the hyperbolic one.

7. Characterization of Bifurcation Diagram and Lyapunov Exponent Graph

Bifurcation diagrams and Lyapunov exponent graphs are fundamental tools for analyzing the behavior of nonlinear dynamical systems. These graphs provide insight into the transitions between dynamical regimes of the system from periodic stability to chaos.

In this case, the analysis takes place for the control parameter ω for variable intervals and for a fixed parameter ($r = 0.5$). The variation of this control parameter changes the way in which the system evolves, leading to either stable steady states, periodic cycles, or chaotic behavior.

7.1. Bifurcation Diagram

The bifurcation diagram shows the stationary values of the dynamic function after the transient effects are removed. It shows how the system solutions evolve as a function of the control parameter.

Related to the bifurcation diagram we can make the following observations:

- i. Bifurcation diagram (Figure 3a):
 - For smaller values of ω (around 1.0–1.5), a “fan-like” structure is observed, which is indicative of stable solutions, starting initially with a point or a slightly deviated orbit, which as ω increases, undergoes successive branching (bifurcations or period doubling).
 - Over larger and larger intervals of ω , the structure becomes denser and denser, with orbits that no longer converge to a limited set of points. This filling of a range of amplitudes indicates a chaotic regime: the orbit is no longer periodic, and the set of points has a fractal character.
 - Occasionally, periodicity windows between chaotic zones can be observed: small intervals of ω in which the system returns to a simpler periodic cycle (orbit of

period 3, 5, etc.), after which, at a small variation of the parameter, it returns to chaos.

ii. Zoom on the bifurcation diagram (Figure 3b,c):

- A zoom (middle and right images) on the intervals 1.8–2.0 and 1.86–1.9, respectively, shows typical structures of chaotic systems with periodic windows. Such windows appear as periodicity windows (short parameter intervals in which the system has a stable periodic orbit).
- Between these windows, the density of the points increases, suggesting a dynamics sensitive to initial conditions. The points no longer tend towards a single stable cycle but appear as multiple, interspersed, branching bands.

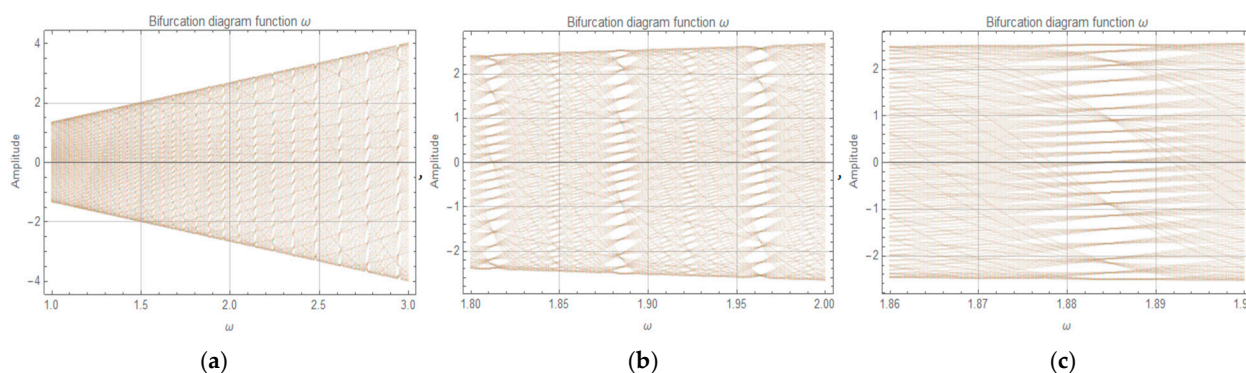


Figure 3. (a–c)—Bifurcation diagram function for: (a) ω between 1.0 and 3.0; (b) ω between 1.8 and 2.0; (c) ω between 1.86 and 1.90.

7.2. The Lyapunov Exponents

The plot of the Lyapunov exponents as a function of ω (for $r = 0.5$, another probable internal parameter of the system) shows how, as ω increases, the Lyapunov exponents become mostly positive (or at least larger than zero)—see Figure 4.

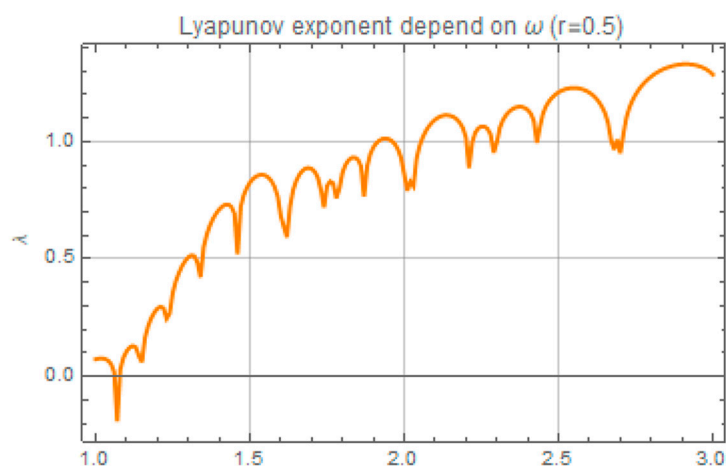


Figure 4. Plot of the Lyapunov exponents as a function of ω .

A positive Lyapunov exponent $\lambda > 0$ indicates chaos, i.e., there is an exponential divergence of trajectories initiated from very close initial conditions. A $\lambda \approx 0$ or negative λ would indicate order or periodicity.

The presented curve has an oscillating shape: there are portions where λ drops below zero, indicating windows of periodicity, and areas where λ is strongly positive, signaling robust chaos. As ω increases towards 3.0, the mean values of λ seem to remain high,

suggesting pronounced and persistent chaos, with short windows of periodic stability (points where sudden decreases in the Lyapunov exponent occur).

From what can be observed, the system exhibits dynamics typical of a transition to chaos through a scale of period-doubling bifurcations. At low values of ω , the system may have a fixed point or a stable periodic orbit.

7.3. Multifractal Characteristics of Chaotic Attractors

In a chaotic regime, the set of points towards which the orbit evolves in-phase space is not a simple one, such as a point or a periodically bounded curve. Instead, the system converges to a chaotic attractor that generally has a fractal or even multifractal geometry. A multifractal attractor is characterized by the fact that different regions of the attractor have different local fractal dimensions, and the extent to which the points of the orbits are distributed on the attractor is non-uniform.

In areas of dense bifurcation (such as those observed for values of ω between 1.8 and 2.0 or finer, between 1.86 and 1.9 in Figure 3b,c), multifractal features become evident: as the parameters change, the structure of the attractor rearranges, the local densities of the distribution of orbits on the attractor change, generating a complex multifractal spectrum.

Positive Lyapunov exponents (0.5–1.5 in large ω ranges) indicate high sensitivity to initial conditions. In an area with $\lambda > 1$, for example, a richer multifractal structure can be expected, as the rapid divergence of the trajectories causes the orbit to “blanket” the attractor in an irregular and non-uniform way. In intervals where $\lambda < 0$ or close to zero (periodic windows), the attractor simplifies, having a fractal dimension close to zero, and lacking the multifractal character.

Between these windows, when reentering chaos, the system again develops a complex fractal attractor. Thus, the value of the fractal dimensions and the multifractal spectrum vary strongly depending on the parameter, giving rise to a complex parametric landscape.

8. Conclusions

The main conclusions of the present paper are the following:

- (i) By assimilating any complex system to a multifractal-type object, it is shown that, in accordance with the Multifractal Theory of Motion, its dynamics can be described through continuous and non-differentiable curves;
- (ii) The covariant derivative is defined and, based on a covariance principle, the specific multifractal momentum conservation law is determined. In such context, the dynamics of any complex system can be separated on differentiable and non-differentiable resolution scales;
- (iii) If the velocities field can be expressed through a gradient, then two scenarios (a Schrödinger-type and a Madelung-type multifractal scenario) become operable;
- (iv) In the Schrödinger-type multifractal scenario, the motion laws are related to the invariant functions of an $SL(2R)$ algebra;
- (v) In the Madelung-type multifractal scenario, the non-differentiable components of the velocity field induce a central-type force;
- (vi) These two scenarios can be correlated, highlighting $SL(2R)$ symmetries and Riccati-type gauges in complex systems dynamics;
- (vii) Correlative dynamics in either of the two scenarios, based on the same $SL(2R)$ symmetry, can be obtained by Stoler coherent states;
- (viii) Several non-trivial dynamics, which imply $SL(2R)$ symmetries through a Riccati-type gauge, are discussed the following: charged particle dynamics in a magnetic monopole (Poincaré monopole), relativistic cosmology in Edington’s sense, and temporal scale variance in Milner’s sense;

- (ix) Our model substitutes constrained dynamics in a usual space with interaction-free dynamics in a multifractal space (in this case, the interaction is taken over by the scale resolution and fractal dimension of the motion curves, just as, in General Relativity, the interaction is taken over by the curvature of space).
- (x) The presented dynamical system, with the bifurcation diagram and the Lyapunov exponent as a function of the parameter ω , shows a classical picture of the transition to chaos, with extensive areas of chaotic regime. Lyapunov analysis shows the existence of many intervals of chaos (positive Lyapunov exponents), interspersed with periodic windows where the Lyapunov exponent drops abruptly (a dynamical regime approaching more ordered dynamics). In chaotic regimes, the asymptotic attractors possess fractal or even multifractal properties. Additionally, the presence of periodic windows interrupting chaotic zones helps to understand the dynamical complexity: the system is not simply chaotic, but has a “fabric” of more ordered/periodic states interposed between chaotic zones, each with its own structural behavior. For example, period doubling can be observed both at microscopic scales and at macroscopic scales [21–23].

Author Contributions: Conceptualization, V.G. and M.A.; methodology, E.N.; software, C.B.; validation, C.P. and D.V.; formal analysis, D.V.; investigation, C.B.; resources, E.N. and C.P.; data curation, C.G.D.; writing—original draft preparation, V.G., C.M.R. and Z.B.; writing—review and editing, D.V. and Z.B.; visualization, C.G.D.; supervision, M.A. and C.M.R.; project administration, V.G. All authors have read and agreed to the published version of the manuscript.

Funding: This research received no external funding.

Data Availability Statement: All the data are presented in the manuscript.

Conflicts of Interest: The authors declare no conflicts of interest.

References

1. Mitchell, M. *Complexity: A Guided Tour*; Oxford University Press: Oxford, UK, 2009.
2. Badii, R. *Complexity: Hierarchical Structures and Scaling in Physics*; Cambridge University Press: Cambridge, UK, 1997.
3. Bar-Yam, Y. *Dynamics of Complex Systems*; CRC Press: Boca Raton, FL, USA, 2019.
4. Estrada, E. What is a complex system, after all? *Found. Sci.* **2023**, *29*, 1143–1170. [[CrossRef](#)]
5. Siegenfeld, A.F.; Bar-Yam, Y. An introduction to complex systems science and its applications. *Complexity* **2020**, *2020*, 6105872. [[CrossRef](#)]
6. Descalzi, O.; Curilef, S.; Velazquez, L.; Muñoz, V. Complex systems and inter/transdisciplinary research: A review. *Chaos Interdiscip. J. Nonlinear Sci.* **2024**, *34*, 010401. [[CrossRef](#)] [[PubMed](#)]
7. Fry, H.M. Complex Systems Dynamics. In *Dynamical and Complex Systems*; World Scientific: Singapore, 2017; pp. 81–120.
8. Boccaletti, S. The synchronized dynamics of complex systems. *Monogr. Ser. Nonlinear Sci. Complex.* **2008**, *6*, 1–239.
9. Merches, I.; Agop, M. *Differentiability and Fractality in Dynamics of Physical Systems*; World Scientific: Hackensack, NJ, USA, 2016.
10. Agop, M.; Paun, V.P. *On the New Perspectives of Fractal theory. Fundamentals and Applications*; Romanian Academy Publishing House: Bucharest, Romania, 2017.
11. Nottale, L. *Scale Relativity and Fractal Space-Time: A New Approach to Unifying Relativity and Quantum Mechanics*; Imperial College Press: London, UK, 2011.
12. Agop, M.; Irimiciuc, S.A. *Multifractal Theory of Motion: From Small to Large Scales*; Springer Nature: Singapore, 2024.
13. Mandelbrot, B.B. *The Fractal Geometry of Nature*; W. H. Freeman and Co.: San Francisco, CA, USA, 1982.
14. Carinena, J.F.; Clemente-Gallardo, J.; Marmo, G. Geometrization of quantum mechanics. *Theor. Math. Phys.* **2007**, *152*, 894–903. [[CrossRef](#)]
15. McDonald, K.T. Birkeland, Darboux and Poincaré: Motion of an electric charge in the field of a magnetic pole. In *E-Print*; Princeton University: Princeton, NJ, USA, 2015.
16. Durham, I.T. Eddington and uncertainty. *Phys. Perspect.* **2003**, *5*, 398–418. [[CrossRef](#)]
17. Verde, L. Statistical methods in cosmology. In *Lectures on Cosmology: Accelerated Expansion of the Universe*; Springer: Berlin/Heidelberg, Germany, 2010; pp. 147–177.

18. Milne, E.A. On the origin of laws of nature. *Nature* **1937**, *139*, 997–999. [[CrossRef](#)]
19. Carinena, J.F.; Ramos, A. Integrability of the Riccati equation from a group-theoretical viewpoint. *Int. J. Mod. Phys. A* **1999**, *14*, 1935–1951. [[CrossRef](#)]
20. Stoler, D. Generalized Coherent States. *Phys. Rev.* **1971**, *D4*, 2309. [[CrossRef](#)]
21. Cheung, P.Y.; Wong, A.Y. Chaotic behavior and period doubling in plasmas. *Phys. Rev. Lett.* **1987**, *59*, 551. [[CrossRef](#)] [[PubMed](#)]
22. Mansuroglu, D.; Uzun-Kaymak, I.U.; Rafatov, I. An evidence of period doubling bifurcation in a dc driven semiconductor-gas discharge plasma. *Phys. Plasmas* **2017**, *24*, 053503. [[CrossRef](#)]
23. Tzuk, O.; Ujjwal, S.R.; Fernandez-Oto, C.; Seifan, M.; Meron, E. Period doubling as an indicator for ecosystem sensitivity to climate extremes. *Sci. Rep.* **2019**, *9*, 19577. [[CrossRef](#)] [[PubMed](#)]

Disclaimer/Publisher’s Note: The statements, opinions and data contained in all publications are solely those of the individual author(s) and contributor(s) and not of MDPI and/or the editor(s). MDPI and/or the editor(s) disclaim responsibility for any injury to people or property resulting from any ideas, methods, instructions or products referred to in the content.